JOURNAL OF PROPULSION AND POWER
Vol. 20, No. 4, July–August 2004

Analytical Development of a Slotted-Grain Solid Rocket Motor

Roy J. Hartfield,* John E. Burkhalter,† and Rhonald M. Jenkins‡
Auburn University, Auburn, Alabama 36849-5338
and
Jay Witt§
Missile Space Intelligence Command, Huntsville, Alabama 35898

In most practical solid-rocket-motor design processes, final designs for grains are determined using computer-generated grids. This process is imminently practical for cases in which small numbers of final geometries are to be considered. However, for a grain design optimization process in which large numbers of grain configurations are to be considered, generating grids for each candidate design is often prohibitive. For such optimization processes analytical developments of burn perimeter and port area for two-dimensional grains are critically important. This paper offers a detailed development of the burn-back equations for a slotted grain with burning only on the slot faces. The result is a set of algebraic equations that can be used to predict burn perimeter and port area at a given burn distance for a given slotted grain design.

Introduction

ANALYTICAL developments for solid-rocket-motor grains were much more prevalent in the decades before widespread use of microcomputers. Development of the burn-back equations for the star grain and one type of wagon wheel can be found in Barrere et al.[1] Most modern texts on solid rocket propulsion[2,3] do not provide geometric details for grain design. A large number of potential grain configurations are described in NASA publications, but very few geometric details are given in such publications.[4,5] Recent advances in the design process for solid rocket motors involve the use of genetic algorithms to evaluate large numbers of potential grain designs to arrive at an optimum solution for the rocket motor.[6–8] The evaluation of large numbers of candidate designs is much more practical if analytical expressions for burn perimeter and port as functions of burn distance are available.

This work describes an analytical development of a slotted solid-rocket-motor grain, suitable for propelling a long, slender rod at high speeds for relatively extended times. In this configuration, the rod would extend through the center of the solid grain, and the maximum diameter of the rocket is relatively small. In such configurations, a large web thickness (and burn time) is difficult to achieve with conventional grain designs. In an effort to extend the burn times, a slotted grain is considered.

Grain Development

Consider a grain situated between two cylindrical case sections with slots cut at even intervals as shown in the schematic present in Fig. 1. The grain burns from the inside of the slots only, and the slots are the only, perforations. The initial slot surfaces are flat and are transformed into partially curved surfaces by the burning of the propellant. The inner cylinder radius is r_i, and the outer cylinder radius is r_o. The burning of the grain is considered to be spatially uniform, and it is assumed that the regression of the grain is normal to the burning surface. It is also assumed that burning occurs only on the surface exposed to the slot.

Three possible burn sequences can occur as follows:

The first phase, which is composed of the flat and curved sections along the inner radius as shown in Fig. 2, can end with the flat burning out. Phase II would then be only the curved section burning and would end when the burning from an adjacent slot is met—at which point phase III would occur. This is referred to as a type I grain. Type I grains occur if the inner radius is a large portion of the outer radius and or only a few slots are present.

The first phase can end prematurely if the burning of one slot is met by the burning of an adjacent slot before the flat burns out. This means that a point is formed from the curved surfaces of the two slots, and this phase II can end by either the curved sections burning out or by the flats burning out. If the flat burns out first, the grain is referred to as a type II. The detailed discussion of this phase along with a figure is included later in the text. The condition for a type II is

$$y_o/r_i > \pi\varepsilon/N \tag{1}$$

where y_o is the maximum perpendicular distance between the initial burning surface and the outer case, r_i is the inner radius, ε is the fraction of the pie-shaped section available for one slot which is filled with grain, and N is the number of slots. These variables are all shown in Fig. 2.

If a type II grain ends phase II with the curves burning out, the grain is a type III. Type II and type III grains exist for small inner radii or large numbers of slots. The condition for a type III is that the grain meet the test for a type II and meet the additional test that

$$y_o/r_i > \tan(\pi\varepsilon/N) \tag{2}$$

All of the conditions for determining phase and all of the equations used to determine burn perimeter and port area are developed as follows.

Phase I Burning

Phase I is the same for all three types of slotted grains. Figure 2 represents the burning of one-half of one slotted section. The angle for a complete slot would be $2\pi/N$, and the angle for half of the slotted section is π/N as shown in the diagram. The diagram is depicted for a value of N of 2, but the derivations are valid for any value of N. The angle θ shown in the diagram is a variable of integration used in calculating the burn perimeter section s_2 and the related port area.

Phase I burning ends at y_o for type I where

$$y_o = \sqrt{r_o^2 - r_i^2} \tag{3}$$

Received 6 March 2003; revision received 2 October 2003; accepted for publication 13 October 2003.

*Associate Professor, Aerospace Engineering.
†Professor, Aerospace Engineering.
‡Associate Professor, Aerospace Engineering.
§Engineer, Aerospace Engineering.

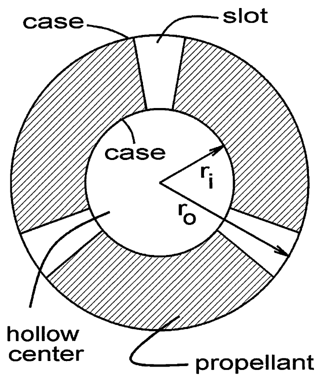

Fig. 1 Schematic of a slot-grain design showing three slots.

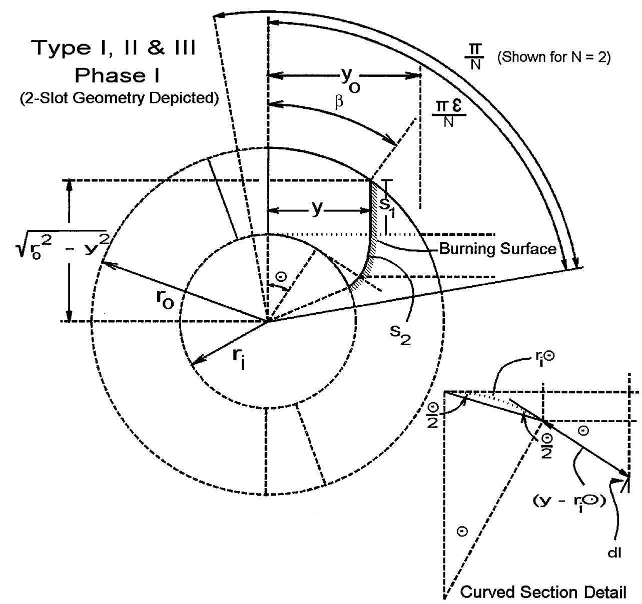

Fig. 2 Schematic showing burn perimeter development for phase I.

and phase I ends for type II for a value of the angle θ of

$$\theta = \pi\varepsilon/N \tag{4}$$

or for a burn distance y of

$$y_{\text{phase II}} = r_i(\pi\varepsilon/N) \tag{5}$$

Burn Perimeters and Port Areas

The following sections are used to show how one-half of the burn perimeter and one-half of the port area for a single slot can be calculated as a function of burn distance y. The expressions will be multiplied by $2N$ to get the total burn perimeters and port areas.

Burn Perimeters for Phase I

The burn perimeter for phase I is composed of the flat section s_1 and the curved section s_2 which goes all of the way from the end of the flat section to the inner cylindrical boundary.

$$s_1 = \sqrt{r_o^2 - y^2} - r_i \tag{6}$$

To get s_2, an integral of dl can be constructed as shown on the right side of Fig. 2. The length dl can be obtained by either constructing a length z, differentiating and dividing by $\cos\theta$, or it can be obtained by recognizing from the drawing that dl is the length of a circular arc of radius $y - r_i\theta$ and angle dθ.

$$\mathrm{d}l = (y - r_i\theta)\,\mathrm{d}\theta \tag{7}$$

This differential is a function of θ only for a given value of y and a given grain design. The curve starts with $\theta = 0$ and ends when

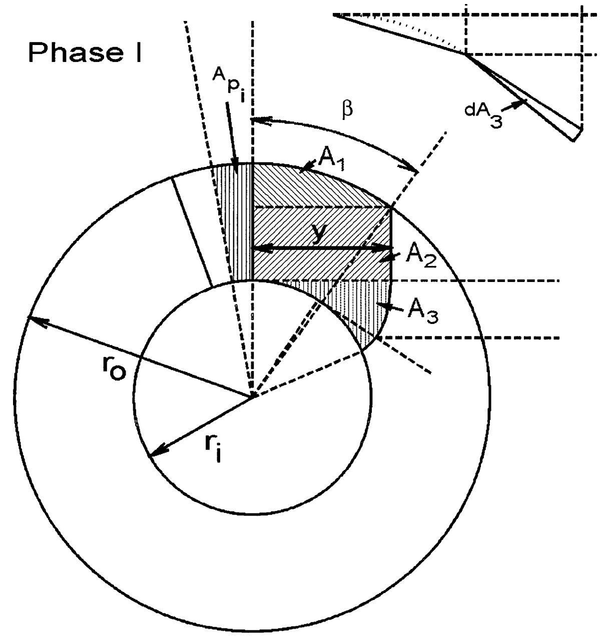

Fig. 3 Schematic for port area calculation for phase I.

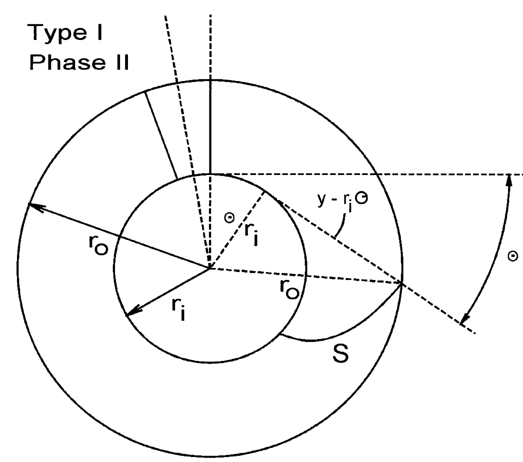

Fig. 4 Burn perimeter for phase II of a type I slot.

$\theta = y/r_i$, and s_2 can be determined by integration as follows:

$$s_2 = l = y\int_0^{y/r_i} \mathrm{d}\theta - r_i\int_0^{y/r_i} \theta\,\mathrm{d}\theta = \frac{y^2}{r_i} - \frac{y^2}{2r_i} = \frac{y^2}{2r_i} \tag{8}$$

Port Area for Phase I

The port area associated with one-half of a slot can be comprised of four sections as shown in Fig. 3. The initial port area can be written as a section of a tube as follows:

$$A_{p_i} = \tfrac{1}{2}(1 - \varepsilon)(\pi/N)\left(r_o^2 - r_i^2\right) \tag{9}$$

The area signified by A_1 is an arc section with a triangle subtracted. The angle for the arc can be written as

$$\beta = \sin^{-1}(y/r_o) \tag{10}$$

and the area A_1 is

$$A_1 = (\beta/2)r_o^2 - (y/2)\sqrt{r_o^2 - y^2} \tag{11}$$

The area A_2 is a rectangle

$$A_2 = s_1 y \tag{12}$$

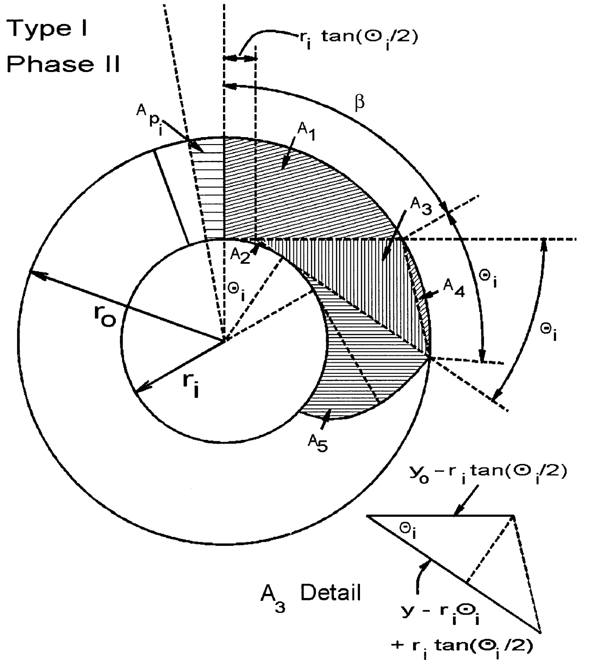

Fig. 5 Port area for phase II in a type I slot (depicted for burning from a single slot).

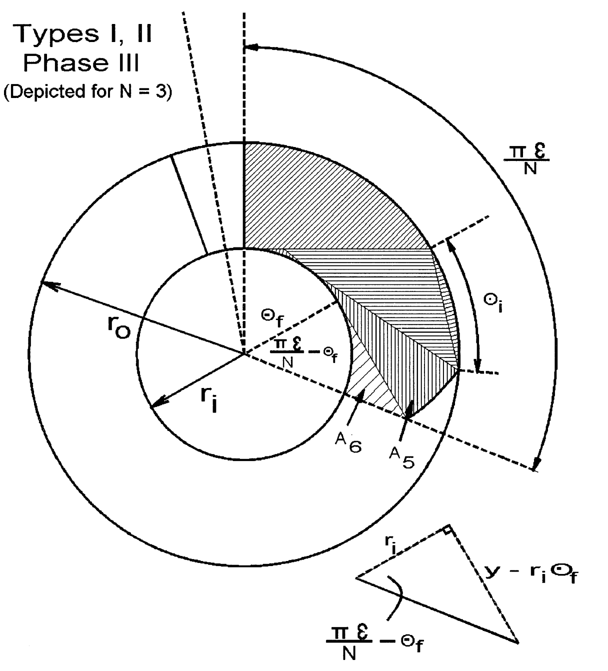

Fig. 6 Phase III slot geometry for type I.

The area A_3 can be obtained by integrating the dA shown. The dA area is an arc section of radius $y - r_i\theta$ and angle dθ.

$$dA_3 = [(y - r_i\theta)^2/2]\,d\theta = \tfrac{1}{2}\left(y^2 - 2yr_i\theta + r_i^2\theta^2\right)d\theta \qquad (13)$$

The limits on θ are still 0 and y/r_i.

$$A_3 = \frac{1}{2}\int_0^{y/r_i}\left(y^2 - 2yr_i\theta + r_i^2\theta^2\right)d\theta$$

$$= \frac{1}{2}\left[y^2\left(\frac{y}{r_i}\right) - yr_i\left(\frac{y}{r_i}\right)^2 + r_i^2\left(\frac{1}{3}\right)\left(\frac{y}{r_i}\right)^3\right] = \frac{y^3}{6r_i} \qquad (14)$$

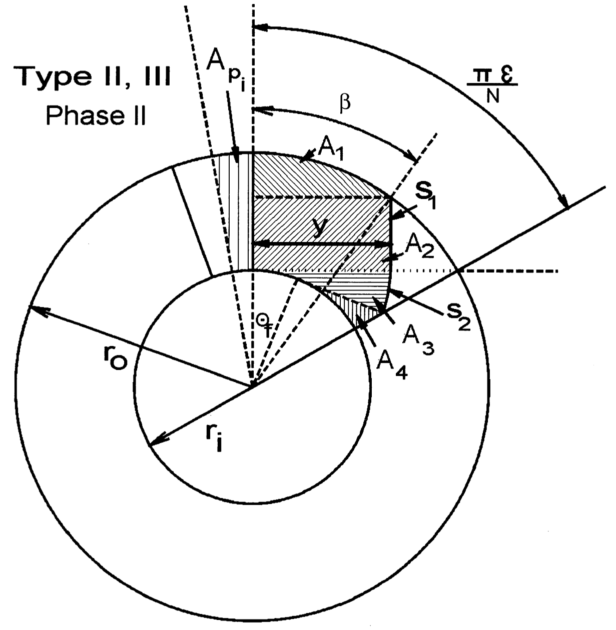

Fig. 7 Phase II geometry for types II and III.

The final port area for one-half of one slot for phase I burning is

$$A_{\text{phase I}} = A_{p_i} + A_1 + A_2 + A_3 \qquad (15)$$

Phase II Burn Perimeter for a Type I Grain

For Phase II burning, only the curved section burns, and it burns from the outer radius all of the way to the inner radius. Phase II for a type I occurs if $y > y_o$.

The differential length is the same as that for the s_2 calculation for phase I. However, the initial value for θ is no longer 0. To get the value for θ_I, refer to the triangle drawn in Fig. 4. The Pythagorean theorem can be written for this triangle and solved for θ_i.

$$r_o^2 = r_i^2 + (y - r_i\theta)^2 \qquad (16)$$

Or

$$\theta_i = \left[y - \sqrt{\left(r_o^2 - r_i^2\right)}\right]\Big/ r_i \qquad (17)$$

The length of the burn perimeter s is then

$$l = \int_{\theta_i}^{y/r_i} (y - r_i\theta_i)\,d\theta \qquad (18)$$

$$l = y\left(\frac{y}{r_i} - \theta_i\right) - \frac{r_i}{2}\left[\left(\frac{y}{r_i}\right)^2 - \theta_i^2\right] \qquad (19)$$

$$l = y\left[\frac{y}{r_i} - \left(\frac{y}{r_i} - \frac{\sqrt{r_o^2 - r_i^2}}{r_i}\right)\right] - \frac{r_i}{2}\left[\left(\frac{y}{r_i}\right)^2 - \left(\frac{y^2}{r_i^2} - \frac{2y\sqrt{r_o^2 - r_i^2}}{r_i^2} + \frac{r_o^2 - r_i^2}{r_i^2}\right)\right] \qquad (20)$$

$$l = y\left(\frac{\sqrt{r_o^2 - r_i^2}}{r_i}\right) - \frac{r_i}{2}\left(\frac{2y\sqrt{r_o^2 - r_i^2}}{r_i^2} + \frac{r_o^2 - r_i^2}{r_i^2}\right) = \frac{r_o^2 - r_i^2}{2r_i^2} \qquad (21)$$

This is the entire burn perimeter for phase II in a type I grain. It is very important to note that this phase of this type is neutral regardless of the design choice.

Port Area for Phase II Burning of a Type I Grain

The port area calculation for phase II is substantially more complex than the phase I port area calculation. Five separate geometric areas are considered and added to the initial port area. The initial port area is unchanged. For the diagram in Fig. 5 the area A_1 is an arc section with a triangle subtracted:

$$A_1 = r_o^2\beta\big/2 - r_i\sqrt{\left(r_o^2 - r_i^2\right)}\big/2 \tag{22}$$

where

$$\beta = \cos^{-1}(r_i/r_o) \tag{23}$$

The area A_2 can be constructed from two right triangles with a circular arc of radius r_i and angle θ_i subtracted.

$$A_2 = 2\left[\left(r_i^2\tan\theta_i\big/2\right)\big/2\right] - r_i^2\theta_i\big/2 = r_i^2\tan\theta_i/2 - \theta_i/2 \tag{24}$$

The determination of θ_i is the same for the area calculation and will be the same for phase III burning. A_3 is a triangle with area of $\frac{1}{2}$ bh.

$$A_3 = \tfrac{1}{2}[(y - r_i\theta_i) + r_i\tan(\theta_i/2)]x[(y_o - r_i\tan(\theta_i/2)\sin\theta_i] \tag{25}$$

A_4 is an arc section with a triangle subtracted from it:

$$A_4 = \tfrac{1}{2}\left(r_o^2\theta_i\right) - [r_o\sin(\theta_i/2)][r_o\cos(\theta_i/2)] \tag{26}$$

It can be shown that the areas A_2, A_3, and A_4 can be combined into the following compact relationship:

$$A_2 + A_3 + A_4 = \tfrac{1}{2}y_o^2\theta_i \tag{27}$$

A_5 is an area that is calculated using the same pie-shaped differential area as that used in the phase I A_3 calculation, but the initial angle for θ is θ_i and not 0.

$$\begin{aligned}A_5 &= \frac{1}{2}\int_{\theta_i}^{y/r_i}\left(y^2 - 2yr_i\theta + r_i^2\theta^2\right)\mathrm{d}\theta\\ &= \frac{1}{2}\left[y^2\left(\frac{y}{r_i}\right) - yr_i\left(\frac{y}{r_i}\right)^2 + r_i^2\left(\frac{1}{3}\right)\left(\frac{y}{r_i}\right)^3\right]\\ &\quad - \frac{1}{2}\left[y^2(\theta_i) - yr_i(\theta_i)^2 + r_i^2\left(\frac{1}{3}\right)(\theta_i)^3\right]\\ &= \frac{y^3}{6r_i} - \frac{1}{2}\left[y^2(\theta_i) - yr_i(\theta_i)^2 + r_i^2\left(\frac{1}{3}\right)(\theta_i)^3\right]\end{aligned} \tag{28}$$

The entire burn area for $\frac{1}{2}$ of 1 slot for a Type I grain in Phase II is

$$A_{\text{Phase II}} = A_{p_i} + A_1 + A_2 + A_3 + A_4 + A_5 \tag{29}$$

Phase III Burning for Types I and II

For both types I and II, phase III consists of burning along part of the curved section that has been explored in detail. The starting angle for this surface is θ_i as was determined for phase II, but the ending angle θ_f is determined from the diagram shown in Fig. 6 using the condition that $\frac{1}{2}$ of a slot can only consume an angle of π/n including the port area where n is the number of slots. The condition to start phase III for a type I grain is $y/r_i > \theta_i/N$. For a type II grain, the condition is $y > y_o$. If $\theta_i > \theta_i/N$, burnout has occurred.

The final angle θ_f can be determined from the triangle using the expression

$$\tan(\pi\varepsilon/N - \theta_f) = (y - r_i\theta_f)/r_i \tag{30}$$

This equation will need to be solved iteratively for θ_f.

The burn perimeter can then be solved from

$$l = \int_{\theta_i}^{\theta_f}(y - r_i\theta_i)\,d\theta \tag{31}$$

$$l = y(\theta_f - \theta_i) - \frac{r_i}{2}\left(\theta_f^2 - \theta_i^2\right) \tag{32}$$

The areas for phase III are the same as the areas for phase II type I, except that the limits on the integration for A_5 are modified and A_6 is added. A_5 becomes

$$\begin{aligned}A_5 &= \frac{1}{2}\int_{\theta_i}^{\theta_f}\left(y^2 - 2yr_i\theta + r_i^2\theta^2\right)\mathrm{d}\theta\\ &= \frac{1}{2}\left[y^2(\theta_f) - yr_i(\theta_f)^2 + r_i^2\left(\frac{1}{3}\right)(\theta_f)^3\right]\\ &\quad - \frac{1}{2}\left[y^2(\theta_i) - yr_i(\theta_i)^2 + r_i^2\left(\frac{1}{3}\right)(\theta_i)^3\right]\\ &= \frac{1}{2}\left[y^2(\theta_f - \theta_i) - yr_i(\theta_f - \theta_i)^2 + r_i^2\left(\frac{1}{3}\right)(\theta_f - \theta_i)^3\right]\end{aligned} \tag{33}$$

A_6 is a triangle with an arc section removed.

$$A_6 = \tfrac{1}{2}(y - r_i\theta_f)(r_i) - \left(r_i^2\big/2\right)(\pi/N - \varepsilon/2 - \theta_f) \tag{34}$$

This concludes all three phases for a type I grain. The only remaining cases are types II and III phase II and type III phase III.

Types II and III, Phase II Burn Perimeter and Port Area

If a grain is in phase I and y/r_i exceeds $\pi/n - \varepsilon/2$, phase II will ensue as shown in Fig. 7.

Burn Perimeter

The length s_1 is calculated exactly as it was in phase I. The distance s_2 is calculated using the same integrand that has been used for the curved section with the limits set at 0 and θ_f, where θ_f is calculated exactly as it was in the third phase of types I and II.

$$s_2 = \int_0^{\theta_f}(y - r_i\theta_i)\,\mathrm{d}\theta = y\theta_f - \frac{r_i\theta_f^2}{2} \tag{35}$$

Port Area

The areas A_1 and A_2 are calculated exactly as they were in phase I. The area A_4 is calculated using the same equation as was used for A_6 in phase III of types I and II. The area A_3 is calculated using the same integrand as was used for the A_5 calculation in phase III but with the lower limit on θ set to 0.

$$\begin{aligned}A_3 &= \frac{1}{2}\int_0^{\theta_f}\left(y^2 - 2yr_i\theta + r_i^2\theta^2\right)\mathrm{d}\theta\\ &= \frac{1}{2}\left[y^2(\theta_f) - 2yr_i\frac{(\theta_f)^2}{2} + r_i^2\frac{(\theta_f)^3}{3}\right]\end{aligned} \tag{36}$$

Type III, Phase III Burn Perimeter and Port Area

For a type III grain, the only burning surface is the flat. A type III rocket exists if y_o calculated in phase I is larger than $r_i\tan(\pi\varepsilon/N)$. From the diagram shown in Fig. 8, the burn perimeter is

$$s = \left[\sqrt{r_o^2 - y^2} - r_i\right] - \frac{y - r_i\tan(\pi/N - \varepsilon/2)}{\tan(\pi/N - \varepsilon/2)} \tag{37}$$

The port area can be considered as an arc section of radius r_o and angle β (where β is calculated exactly as in phase I) and a triangle with an arc section of radius r_i and angle $\pi\varepsilon/N$ removed.

$$A_1 + A_2 = r_o^2\beta\big/2 + \tfrac{1}{2}s_1r_o[\sin(\beta)] - \tfrac{1}{2}r_i^2(\pi\varepsilon/N) \tag{38}$$

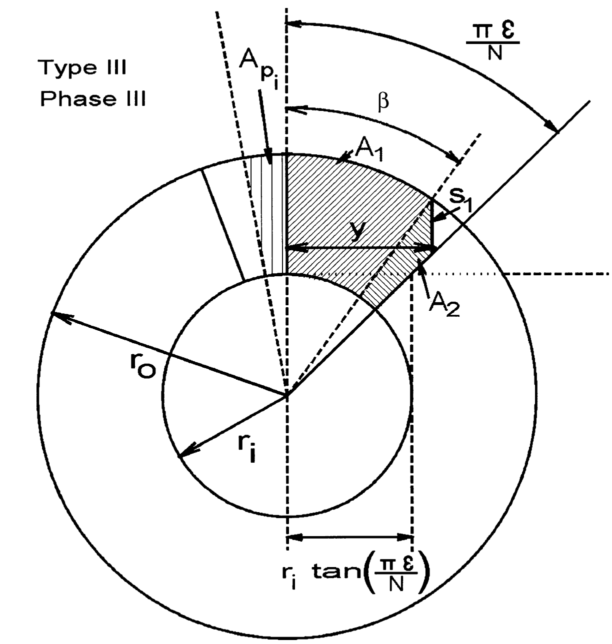

Fig. 8 Phase III geometry for a type III.

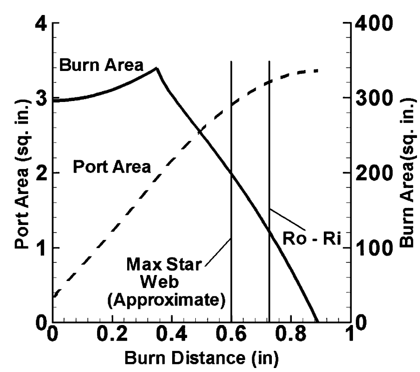

Fig. 9 Burn distance and port area for a three-slot grain with R_i = 0.375 in. (0.95 cm), R_o = 1.1 in. (2.8 cm), ε = 0.9, and grain length = 68 in. (173 cm).

For this mode, burnout occurs for $s_1 = 0$. This leads to a burnout condition as follows:

$$y = r_o \sin(\pi\varepsilon/N) \tag{39}$$

Web Thickness

The web thickness for this slotted-grain design can be calculated for types I and II using an arc for an angle $\theta_{\text{End Burn}}$, and a straight section is y_o, where $\theta_{\text{End Burn}}$ can be determined using the equation

$$\pi\varepsilon/N - \theta_{\text{End Burn}} = \cos^{-1}(r_i/r_o) \tag{40}$$

or

$$\theta_{\text{End Burn}} = \pi\varepsilon/N - \cos^{-1}(r_i/r_o) \tag{41}$$

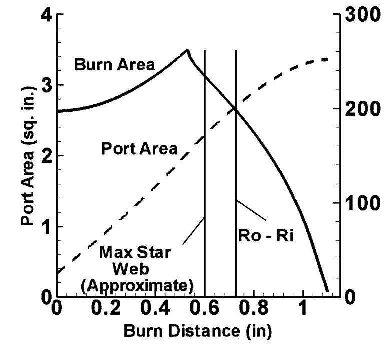

Fig. 10 Burn distance and port area for a two-slot grain with R_i = 0.375 in. (0.95 cm), R_o = 1.1 in. (2.8 cm), ε = 0.9, and grain length = 68 in. (173 cm).

The equation for the web thickness is then

$$\text{web} = y_o + r_i\theta_{\text{End Burn}} \tag{42}$$

For a type III grain, the web thickness is given by

$$\text{web} = r_o \sin(\pi\varepsilon/N) \tag{43}$$

To illustrate the idea that the slot can potentially provide a larger web thickness than those possible with conventional *cp* star or wagon-wheel grains, the plots shown in Figs. 9 and 10 showing burn area vs burn distance have been constructed. Notice that the burn area is substantial for the slotted grain, well beyond the maximum web thickness for a star grain geometry, for this type of a rocket motor configuration. The longest possible burn distance occurs for a minimum number of slots.

Conclusions

This paper offers a detailed development of the burn-back equations for a slotted grain with burning only on the slot faces. The result is a set of algebraic equations that can be used to predict burn perimeter and port area at a given burn distance for a given slotted grain design.

References

[1]Barrere, M., Jaumotte, A., Veubeke, B., and Vandenkerckhove, J., *Rocket Propulsion*, Elsevier, Amsterdam, 1960.

[2]Davenas, A., *Solid Rocket Propulsion Technology*, Pergamon, Oxford, England, UK, 1993.

[3]Sutton, G., and Biblarz, O., *Rocket Propulsion Elements*, 7th ed., Wiley, New York, 2001.

[4]"Solid Propellant Grain Design and Internal Ballistics," NASA SP 8076, URL: library.msfc.nasa.gov/cgi-bin/lsp8000.

[5]"Solid Rocket Motor Performance Analysis and Prediction," NASA SP 8039, URL: library.msfc.nasa.gov/cgi-bin/lsp8000.

[6]Anderson, M., Burkhalter, J., and Jenkins, R., "Design of a Guided Missile Interceptor Using a Genetic Algorithm," *Journal of Spacecraft and Rockets*, Vol. 38, No. 1, 2001, pp. 28–35.

[7]Anderson, M., Burkhalter, J., and Jenkins, R., "Missile Shape Optimization Using Genetic Algorithms," *Journal of Spacecraft and Rockets*, Vol. 37, No. 5, 2000, pp. 663–669.

[8]Anderson, M. B., Burkhalter, J. E., and Jenkins, R. M., "Intelligent Systems Approach to Designing an Interceptor to Defeat Highly Maneuverable Targets," AIAA Paper 2001-1123, Jan. 2001.